SIN-CHN SCIENTIFIC PRESS PTE.LTD.

Molecular & Cellular Biomechanics 2025, 22(3), 1049.
https://doi.org/10.62617/mcb1049

Article

Multivariate emotional AI model for enhancing students' ideological education and mental health via brain-computer interfaces and biomechanics

Yu Zhao

Northeast Agricultural University, Harbin 150030, China; neau_zhaoyu2005@163.com

CITATION

Zhao Y. Multivariate emotional AI model for enhancing students' ideological education and mental health via brain-computer interfaces and biomechanics. Molecular & Cellular Biomechanics. 2025; 22(3): 1049. https://doi.org/10.62617/mcb1049

ARTICLE INFO

Received: 9 December 2024
Accepted: 10 February 2025
Available online: 27 February 2025

Abstract: This paper investigates attention fatigue detection and multi-grain emotional AI classification for student mental health through an educational brain-computer interface (BCI), with a focus on integrating biomechanical principles to enhance understanding and application. Recognizing the growing importance of students' mental health and well-being, this study introduces a domain generalization approach in transfer learning to improve cross-subject BCI model accuracy, addressing the challenges of individual variability. The proposed model utilizes only seven electrodes and achieves a 90% accuracy rate in differentiating between two cognitive-behavioral tasks. A truncated weighting algorithm is employed to optimize electrode combinations, enabling effective generalization across subjects. To tackle the practical challenges of emotion recognition in educational settings, the study reduces data sampling points by identifying key brain regions and frequency bands associated with emotions. Machine learning algorithms, including support vector machines (SVM), Bayesian networks, and K-nearest neighbor (KNN), further enhance recognition accuracy. By integrating eye movement and electroencephalography (EEG) signals using deep canonical correlation analysis, the model achieves cumulative accuracy improvements of 15% and 12% compared to unimodal EEG and eye movement data, respectively, across 12 subjects. Incorporating biomechanical principles, the study also examines the mechanical properties of neural tissues and their influence on signal propagation. By analyzing the viscoelastic behavior of brain tissue and its impact on EEG signal transmission, the research provides insights into how mechanical stress and strain affect neural activity. This biomechanical perspective enhances the understanding of individual variability in EEG signals and contributes to the development of more robust and personalized BCI models. The integration of biomechanics with AI-driven emotion classification and attention fatigue detection offers a comprehensive approach to improving student mental health and educational outcomes. This fusion approach demonstrates superior performance in both emotion classification and attention fatigue detection, offering substantial potential for real-time interventions in student mental health and the enhancement of educational outcomes.

Keywords: brain-computer interface; attention fatigue detection; biomechanics; student mental health; emotion recognition; AI classification; educational BCI

1. Introduction

Emotions are integral to human experience, serving as continuous or discontinuous responses to internal and external stimuli and playing a crucial role in the survival of living beings. Typically, emotions are short-lived yet complex, involving verbal, physical, and behavioral responses that significantly influence an individual's daily life, including social interactions. From a medical perspective, assessing a patient's emotional state during treatment or hospitalization can significantly aid recovery and

guide effective treatment planning [1]. Furthermore, portable emotion recognition technology with communication capabilities can facilitate real-time detection of emotional states, improving mental health monitoring [2].

Non-verbal cues, such as head posture and eye gaze, are critical forms of communication, especially in specific contexts. For example, commercial companies analyze consumers' attention and feedback using gaze tracking, researchers measure child development using head posture estimates, and car manufacturers monitor drivers' head posture and gaze to develop advanced driver assistance systems. In educational settings, tracking students' attention can help improve teaching quality [3,4]. However, despite progress in gaze and head pose estimation, real-world factors such as lighting changes, occlusion, and motion blur continue to challenge algorithm performance [5].

Emotion computing research typically focuses on three main areas: emotion recognition, emotion expression, and emotional decision-making. Among these, emotion recognition is the most critical as it enables machines to accurately understand a human's emotional state. This process often involves analyzing behavioral or physiological signals, such as electroencephalography (EEG), both of which convey valuable emotional information [6]. Behavioral signals, often expressed subconsciously, are a primary means of communicating emotions and feelings to others. They are direct, convenient, and require minimal equipment [7].

Among physiological signals, EEG is one of the most reliable methods for emotion recognition, as it directly reflects brain activity. Emotions are mental responses generated by the brain in reaction to external stimuli, and distinct emotions produce unique EEG signals across various cortical regions. Therefore, EEG objectively represents emotional states [8]. While EEG suffers from poor spatial resolution—requiring numerous electrodes to be placed on the scalp—it offers excellent temporal resolution, making it suitable for studying changes in emotional states over time [9]. Modern wireless EEG devices, being non-invasive, portable, and practical, add value to real-world applications in emotion recognition, particularly in brain-computer interfaces (BCIs) [10].

Feature extraction is critical in emotion recognition, as it involves isolating meaningful information from EEG signals for classification purposes. Due to the high dimensionality of EEG data, direct processing is challenging. Extracting key features to create vectors simplifies emotion classification tasks [11]. Emotions arise from synergistic activity across the cerebral cortex, limbic system, and subcortical processes [12]. Therefore, EEG-based emotion recognition must account for these synergistic relationships between brain regions. Traditional feature extraction methods often rely on single-lead electrodes, overlooking spatial correlations between electrodes. Recently, convolutional neural networks (CNNs) have been utilized to extract spatio-temporal features, enhancing model performance [13].

In deep neural network-based emotion recognition, spectral maps are frequently used for feature extraction. CNNs trained on temporal and frequency axes significantly enhance accuracy by merging information from both axes and feeding it into long short-term memory (LSTM) networks [14]. Significant advancements have been made in emotion recognition and fatigue detection, employing a variety of monitoring methods and channels. While EEG-based approaches are considered objective, alternative methods continue to drive innovation [15].

In ergonomics, muscle fatigue detection is another important application. Fatigue is often assessed by comparing surface electromyography (sEMG) data with maximum voluntary contraction capacity [16]. In human-computer interaction (HCI), hybrid systems combining multiple modalities, such as EEG and sEMG, have proven effective for control purposes [17]. Hybrid modalities leverage the distinct time-frequency characteristics of EEG signals to improve control [18]. Additionally, EEG can mitigate the adverse effects of muscle fatigue in sEMG systems [19].

Head pose estimation is another critical component of computer vision that shares methodologies with other vision tasks. Feature extraction from facial images typically employs local and global approaches. However, global feature extraction methods are prone to performance degradation due to occlusion or lighting changes, while local methods require high-quality images [20]. In recent years, the availability of diverse head pose datasets has facilitated algorithm training and testing, yet real-world performance remains a challenge [21–27].

This paper investigates the use of EEG and other bioelectrical signals for emotion recognition and attention fatigue detection, with a particular focus on educational brain-computer interfaces. The following sections review existing research, describe the proposed model, present experimental results, and conclude with a summary of key findings.

2. Brain-computer interface attention fatigue detection for mental health multi-grain emotional AI classification analysis

2.1. Brain-computer interface attention detection design

In the human brain, billions of neurons maintain electrical charges. Membrane transporter proteins polarize and charge neurons, facilitating the continuous exchange of ions with the extracellular environment. Similarly charged ions repel each other, and when many neurons simultaneously release ions, the resulting movement of surrounding ions can be driven by repulsion. This iterative process is known as volume conduction. If a person is wearing an EEG cap, the ion waves generated through volume conduction can push electrons within the metal electrodes as they reach the scalp. By measuring the potential difference between any two electrodes, a corresponding voltage map can be created. This time-transformed map of voltage differences constitutes the electroencephalogram (EEG) [28].

The potentials generated by a single neuron are too small to be detected by EEG. Therefore, EEG signals always reflect the summed and synchronized activity of thousands or millions of neurons with similar spatial orientation [29]. Because the gradient of the voltage field decreases with the square of the distance, activity originating from deep brain regions is more challenging to detect than currents near the skull. Scalp EEG recordings display oscillations across various frequency bands. Each frequency band corresponds to specific intervals and is associated with different brain states and functions [30].

Research measuring EEG signals and neuronal spiking has revealed a complex relationship between the two. Among these findings, EEG power in the Gamma band

and phase in the Theta band have been shown to correlate most strongly with neuronal spiking activity, as illustrated in **Figure 1** [31].

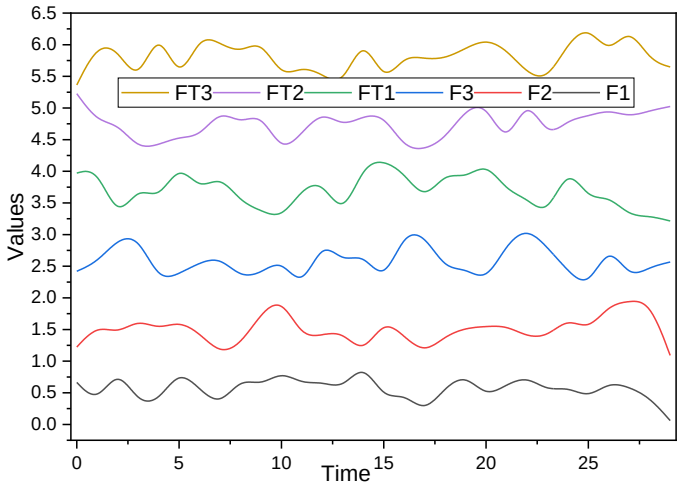

Figure 1. EEG signal.

After the EEG signal features are extracted, the next step is the pattern recognition of the feature signals. A machine learning algorithm is used to classify the extracted feature values, and the classification accuracy represents the success of the analysis results. EEG signals, which refer to the electrical signals collected from the brain cortex, are susceptible to interference from non-cortical sources, commonly referred to as noise. Noise in EEG signals generally comes in three forms: ocular, cardiac, and electromyographic noise, along with interference from the external environment. Among these, interference caused by blinking movements is particularly prominent [32]. Attempts to reduce such interference involve minimizing eye and surrounding tissue movement, yet blinking occurs several times a minute, and eye rotation is inevitable, severely affecting the quality of the EEG signal [33].

The neurobiological explanation of human emotion, particularly concerning the relationship between the nervous system and the limbic system, posits that emotions are pleasurable or non-pleasurable states originating in the limbic system of mammals [34]. If mammals are considered separately from reptiles, emotions become more distinctive in mammals, largely influenced by neurochemicals such as dopamine, norepinephrine, and serotonin, which modulate brain activity levels. These chemical changes are often reflected through body movements, gestures, and postures [35]. For example, emotional states such as love, particularly in terms of care, feeding, and offspring rearing, were proposed as central to mammalian emotional expressions, which developed in older cortical regions. As nocturnal mammals emerged, the sense of smell replaced vision as the dominant sensory input, and the different response patterns triggered by smell are thought to have evolved into mammalian emotions and emotion-related memories [36].

The mammalian brain's reliance on olfactory input is believed to have provided a significant evolutionary advantage, particularly over reptiles during nocturnal hours. The large olfactory bulbs in mammals likely facilitated the development of the limbic system, a key component in processing emotions [37]. The mammalian brain's ability to dominate in nocturnal conditions is attributed to these enlarged olfactory pathways,

which formed the basis of the neural networks that later developed into the limbic system and contributed to the evolution of complex emotional responses.

As shown in **Figure 2**, electromyography (EMG) signals assess muscle function by recording signals from electrodes placed on the skin surface. These electrodes can be classified into wet and dry electrodes based on the conductive medium used. Wet electrodes, similar in material and structure to EEG electrodes, include a pre-prepared conductive paste that can be directly applied near the muscles to be recorded during experiments. To ensure stable contact and meet the high input resistance requirements of the acquisition system, the skin is usually cleaned before placing wet electrodes. On the other hand, dry electrodes, with higher input impedance, are not affected by skin-electrode contact resistance during acquisition, making them more convenient for usage [38,39]. Electrodes can also be categorized as resistive or capacitive, based on how they couple with the skin. Capacitive electrodes, while easier to apply, tend to generate more noise, requiring the addition of analog filtering circuits to improve signal quality during acquisition [40].

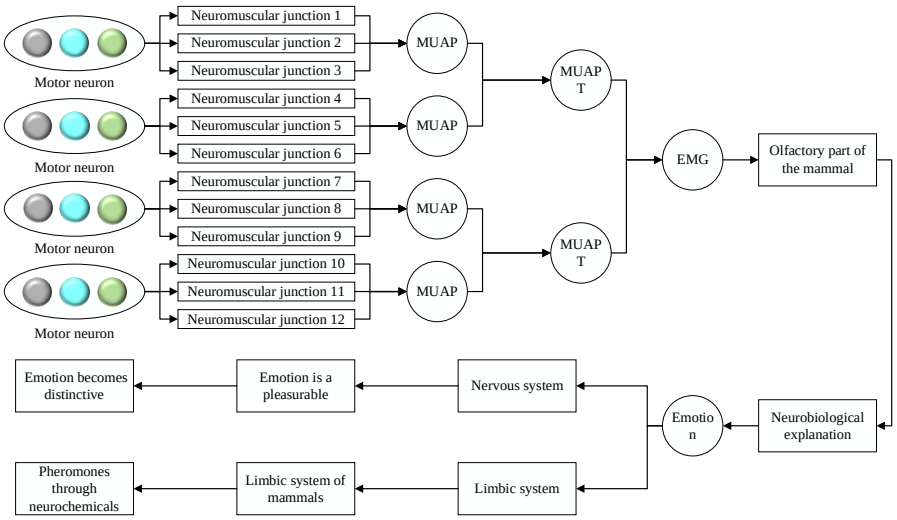

Figure 2. sEMG signal generation and linear system structure.

In terms of data analysis, EMG signal features can be classified into first-order to fourth-order statistics. First-order statistics include basic statistical measures such as the arithmetic mean, absolute mean, and waveform length. Second-order statistics represent the variability in the signal, encompassing parameters such as variance, the number of waveform sign changes, and energy percentage. Third-order statistics, such as skewness, describe the asymmetry in the signal's distribution, while fourth-order statistics, such as kurtosis, describe the sharpness of the signal peaks [41,42].

The absolute value means MAVk is estimated by summing up the absolute values of all points xi in the kth sEMG signal segment and dividing them by the length N of the segment, which is calculated as shown in Equation (1).

$$MAV_k = \frac{1}{N}\sum_{i=1}^{N} x_i^2 \tag{1}$$

The human body is a bad conductor, and the human body resistance is equated to R_1 with a resistance of approximately 2 kΩ to 20 MΩ. The input impedance of the

acquisition system is R_{in}, and if the signal collected from the skin surface is V_{EMG}, the sEMG signal V_{in} entering the acquisition system is:

$$V_{\text{in}} = V_{\text{EMG}} \times \frac{R_{\text{in}}^2}{R_{\text{in}} + R_1} \tag{2}$$

According to the limit theorem, an input signal close to the original signal can be extracted only when the input impedance tends to infinity [43]. In practice, the input impedance of the sEMG signal amplifier must be at least two orders of magnitude greater than the electrode-skin impedance, and an input impedance greater than 100 MΩ is generally considered ideal [44].

Differential mode interference in the system requires the design of analog filtering circuits to eliminate it. Both hardware circuits and software algorithms use a high-pass filter with a 3 dB cutoff frequency in the range of 10–20 Hz and a low-pass filter with a 3 dB cutoff frequency in the range of 400–450 Hz to avoid losing useful information during the processing of sEMG signals [45]. The offline system design uses the AD8626 chip to build the analog filter. Considering system power consumption and design cost, the fourth-order Butterworth low-pass filter and the second-order high-pass filter are selected for this study [46]. Additionally, the highly integrated active filter UAF42 is used to form a dual T-shaped 50 Hz interference filter circuit, which effectively reduces interference from the power line frequency [47,48].

2.2. Analysis of mental health multi-granularity affective AI classification model design

These 3 feature vectors were averaged and used as the baseline signal differential entropy features of the subject before each viewing of a particular emotional video. Finally, the difference between the differential entropy feature of the experimental signal (the EEG signal generated when the subject is stimulated by the emotional video) and the differential entropy feature of the baseline signal is used to represent the emotional state feature of each EEG segment. This process can be expressed as in Equation (3).

$$\text{final\_}v_j^i = \text{exper\_}v_j^i + \frac{\sum_{k=1}^{3} \text{base\_}v_k^i}{4} \tag{3}$$

where $\text{exper\_}v_j^i$ denotes the differential entropy feature vector of the EEG signal in frequency band in the *j*-th experimental signal fragment; $\text{base\_}v_k^i$ denotes the differential entropy feature vector of the EEG signal in frequency band *i* in the *k*-th baseline signal fragment; $\text{final\_}v_j^i$ is the final emotional state feature vector after considering the baseline signal.

In image tracking of a window for a face target in the next video frame search image, the parameters of the current video frame search window are reset and initialized using the second-order value of the obtained search window with the second-order moment of the search window as:

$$M_{11} = \sum_x \sum_y xyI(x, y), M_{20} \tag{4}$$

The collected material needs to be screened through multiple clips. Since the Valence-Arousal two-dimensional affective model was chosen for this experiment, the classification of affective states is determined based on different values of Arousal and Valence. To ensure high-quality emotional evocation, clips with low recognition are removed, and only those with strong emotional impact are selected. Each video clip is evaluated along two dimensions: Arousal and Valence. Both Arousal and Valence have 9 possible values, with Valence value 1 representing the lowest level of pleasure and Valence value 9 representing the highest. Meanwhile, Arousal value 9 represents the highest level of Arousal, and Arousal value 1 represents the lowest [49].

For classification purposes, clips where both Valence and Arousal values exceed 5 are considered to evoke a positive affective state. The assessment results from each participant involved in screening the emotional material are compiled. Only those clips with significant emotional evocation and the highest consistency among participants are retained as the final experimental material, as illustrated in **Figure 3** [50,51].

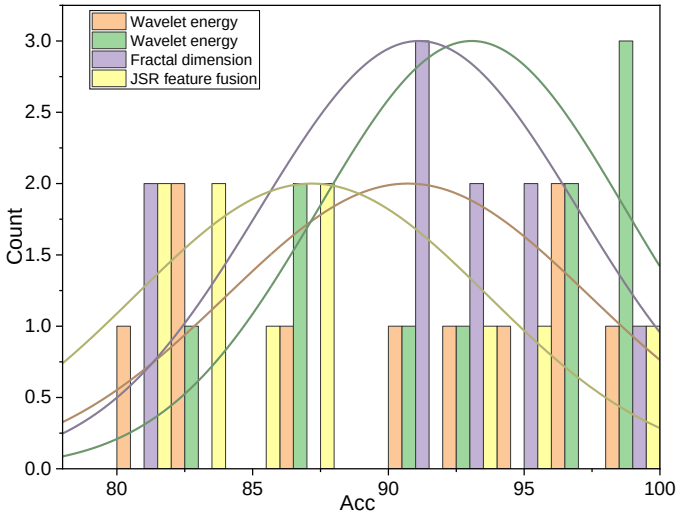

Figure 3. Emotion recognition for different features.

Classification accuracy is the most used evaluation metric when evaluating classification tasks, but in the case of unbalanced data distribution, the accuracy may not objectively reflect the performance of the classifier. When the classification has different error generations, the accuracy only ensures the minimum number of errors, but not the minimum total cost. In various applications of classification, where classifiers are required to prove their reliability, accuracy has been shown to have some shortcomings and deficiencies in current applications. The confusion matrix can schematically visualize the classification results and is used to represent the relationship between the actual and predicted categories of the test data.

The principal component analysis first calculates the correlation matrix of the variable matrix, and the cumulative variance contribution ratio is calculated from the correlation matrix eigenvalues *ji* to replace the variance to measure the amount of information carried, and the principal components are determined by the eigenvectors of the correlation matrix. Let *p n*-dimensional characteristic variables constitute the original data matrix *X*. The calculation steps are as follows:

$$X = \begin{bmatrix} X_{11} & X1p \\ X_{n1} & X_{np} \end{bmatrix} \tag{5}$$

The raw data are normalized to obtain the normalization matrix Y. The information entropy of the label y is calculated, which is a measure of uncertainty; the smaller the probability of an event occurring, the higher the uncertainty.

$$H(y) = \sum_{i=1}^{N} p(y_i) \ln p\,(y_i) \tag{6}$$

Given a variable X, the degree of uncertainty in the variable y can be expressed in terms of conditional entropy as

$$H(y|X) = \sum_{i=1}^{N} \frac{1}{N} p(y_i|x_1) \ln p\,(y_i|x_1) \tag{7}$$

To better describe the general connection between things, the concept of mutual information is introduced, which indicates the degree of association between random variables, $X'_{(i,W_{\min})}$ and y. The mutual information between $X'_{(i,W_{\min})}$ and y is:

$$MI = I\left(X'_{(i,W_{\min})}, y\right) \tag{8}$$

The data matrix of length MIW and with the highest mutual information $X'_{(i,W_{\min})}$, $qMI \in \left[1,2,\ldots,K_{W_{MI}}\right]$ is the final simplified data matrix [19]. It is assumed that the simplified data matrix with the highest mutual information contains signals with the highest emotional intensity that are selected for further analysis, as shown in **Table 1**.

Table 1. Multi-grain sentiment AI classification.

Input	**The parameters are entered, $\lambda, \varepsilon, m \gg n$, the sample set $S^i = \{(x_l^i, y_l^i)\}_{l=1}^{n_i}$**
Output	1: Calculate Gram matrix K and L
	2: DICA: $C = L(L - N \in I)^{-2}K^2$
	3: According to, $\frac{1}{n}CB = KQK - K - \lambda I\ BT$ to calculate the conversion matrix B
	4: output B

We next discuss intra-class scattering and inter-class variation. Here we use $l \in \{1,\ldots,C\}$ to denote the conditional probability distribution $P_{X|l=1}$ over the space $\mathcal{X}$ for the co-C class labels, which should be on the joint distribution P_{XY} educed from P_{XY}. Based on the above conditions, the inter-class scatter is defined as:

$$\psi\left(\left\{\mu_{P_{X|l=1}},\ldots,\mu_{P_{XC}}\right\}\right) = 1 \tag{9}$$

The intra-class scatter of class l is defined as:

$$\psi(P_{XY}) = 1 \tag{10}$$

Suppose the set of samples of class l after a nonlinear mapping ϕ is $SS_{lw} = \{\phi(x_i)\}_{y_i=l}$, then the centroid of the class l mapping sample set is $\mu l = \frac{1}{N} l \sum\{\phi(x_i)\}_{y_i=l}$, where *Nl* denotes the number of samples in category *l*.

In each of the kernel function-based algorithms involved in the experiments, we used linear kernel functions for computation. For algorithms such as Transfer Component Analysis (TCA) that require large-scale matrix operations, we simplify the operations by employing a downsampling method. Specifically, 1000 samples are randomly selected from each source domain subject and pooled together as the training set due to memory and operational constraints. Since each algorithm involves extensive hyperparameter searches, we ensure a wide search range to accommodate sufficient hyperparameter adjustments [52].

However, none of the five algorithm combinations based on the FCSP (Filter Common Spatial Patterns) algorithm mentioned in the previous section simultaneously consider both metrics. Algorithms such as EC (Electrode Combination) and Corer-Feat can measure the similarity between feature vectors but do not account for the direct effect of the classifier on electrode selection. The DM (Distance Metric) algorithm measures the distance between similar and dissimilar samples in Euclidean space, calculating the separability of each electrode, and then combines classification results to obtain the optimal small number of electrode combinations. However, practical analysis shows that adding electrodes according to separability rankings does not always enhance classifier performance and may lead to performance fluctuations [53].

The FCSP + SVM (support vector machines) + probability distribution matrix (Corr-Prob) approach calculates the relationship between single-electrode classification results and all-electrode classification results, essentially using the performance of single-electrode classifiers as a direct criterion for the separability metric. This approach ensures a more balanced electrode selection process, reducing performance fluctuations, as shown in **Table 2** [54–57].

Table 2. Detailed flow of the algorithm and pseudo code.

Input: EEG signal containing all electrodes
Output: Sorted list of electrode separability **R**
Process:
Step 1: Initialize. Initialize an empty list **R** used to record the sorting of electrode separability; initialize another list **S** representing the current electrode subset state (which specific electrodes are included), and the initial state should include all electrodes.
While S ≠ O do
Step 2: Calculate the separability ranking. According to Equation (4), calculate the separability standard J_{ef} of each electrode in the current electrode subset S, and sort in reverse order according to J_h.
Step 3: Eliminate the electrode with the worst separability. According to the current separability ranking, the electrode with the worst separability (assumed to be Ch_1) is eliminated, and the electrode subset S_1 after Ch_1 is eliminated.
Step 4: Testing and comparison of classification performance. For the **S** and S electrode subsets, the FACP and SVM algorithms respectively extract feature vectors and classify them to obtain the classification accuracy index.
The classification performance **if** St_1 is better than S **do**
To achieve the purpose of the algorithm, write Ch to the list **R**, remove Ch from S, and re-assign S to O. The classification performance of **elif S** is better than S_1 **do**

Table 2. (*Continued*).

Input: EEG signal containing all electrodes
Calculate the correlation between the Ch feature vector and the feature vector of the S electrode subset r, calculate the Metropolis criterion according to Equation (5)
if (criteria condition is true) and (r is less than the threshold) do
Write Ch to list R, remove Ch from S, and re-assign S_1 to O.
end if
Return R

When the electrode selection process is first started, there should be a higher probability of re-evaluating the removed electrodes because of the influence of noise and other factors that make the algorithm inaccurate for electrode separability assessment, and the probability of re-evaluation should be reduced when the remaining electrodes are gradually reduced [20]. Therefore, the Metropolis criterion as in Equation (11) is defined based on the application of the SA algorithm to the electrode selection of the BCI system.

$$\exp\left(\frac{\gamma * (\mathrm{Acc}(i) + \mathrm{Acc}(j))}{\mathrm{leftNumber}}\right) \leq \mathrm{random}(0,1) \tag{11}$$

where $\mathrm{Acc}(i)$ and $\mathrm{Acc}(j)$ represent the state of the electrode combination eigenvectors (classification performance metrics) before and after excluding the corresponding electrodes, respectively, leftNumber is the number of electrodes in the remaining subset, $\mathrm{random}(0,1)$ represents the random function that models the acceptance probability of the Metropolis criterion, and γ is a hyperparameter that is set to 1000 in this thesis work.

3. Analysis of results

3.1. Brain-computer interface attention detection results

In online learning scenarios, students are typically seated close to screens—whether on computers, tablets, or other electronic devices—resulting in minimal head deflection when they are focused on learning content. In this chapter's experimental analysis, it is assumed that when the deflection angle of a learner's head in the image exceeds ± 45°, the system detects the student's head as being in a deflection state within the current frame [58].

After the lesson, in-depth interviews were conducted with both lecturers and students to comprehensively evaluate the accuracy of the student classroom attention detection system. Teachers compared the system's evaluation results with students' performance in stage exams. The analysis revealed that the system demonstrated strong predictability regarding students' learning performance, with high accuracy in its identification results, highlighting its valuable potential for practical application [59].

Interviews with students further confirmed the system's reliability. When students reviewed video replays after class, they found the system's evaluations consistent with their actual learning states at the time, providing additional evidence of its high accuracy [60]. Both teachers and students agreed that the student classroom

attention detection system was user-friendly and made a significant contribution to classroom teaching, as illustrated in **Figure 4** [61–64].

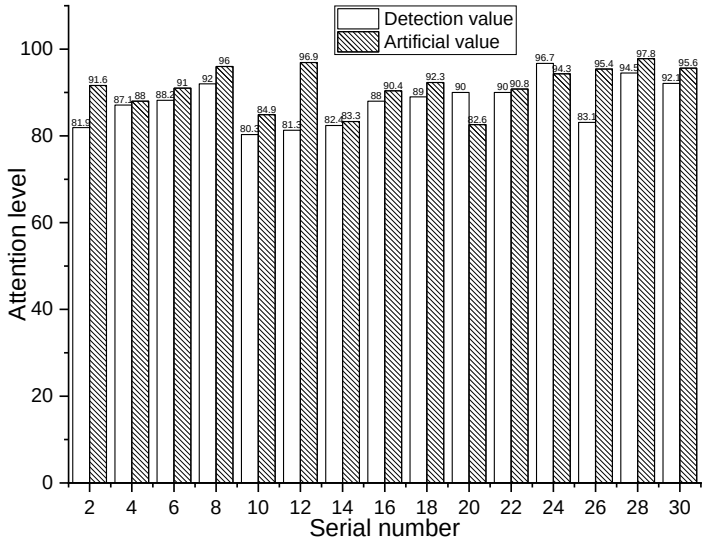

Figure 4. Comparison of attention levels.

The experimental results demonstrate that the method proposed in this paper aligns closely with manual statistics, achieving a 92% accuracy rate for the student classroom attention evaluation detection system. In follow-up experiments, detecting students' attention under normal lighting conditions yielded a 2.5% improvement in detection accuracy. This further validates the effectiveness of the proposed method in detecting classroom learning behaviors. The system serves as a valuable process evaluation tool, allowing teachers to comprehensively monitor classroom content and students' learning behaviors. By enhancing the quality of teaching, this method shows significant potential for practical application in classroom settings [65].

Additionally, a line-of-sight estimation method based on a compound loss convolutional neural network (CNN) was implemented. This novel approach introduces a compound loss model with a spatial weighting layer. The network utilizes two independent fully connected layers to predict the horizontal and vertical deflection angles of the line of sight. Each angle is assigned its own loss function, which is further divided into two components: angle classification and regression. The models were trained and optimized using the dataset, and comparative experiments with previously superior models revealed that this CNN-based line-of-sight estimation method delivers excellent performance and generalization capabilities. Ablation studies conducted on several components of the compound loss further confirmed the effectiveness of the proposed method [66,67].

Given that instances of distraction were less frequent and the study involved a relatively homogeneous sample of students, a shorter observation period was allocated for distracted states. During testing, students were instructed to remain in a focused study state for the first 30 s of the video. Afterward, they were asked to perform random actions such as looking left or right, leaving their seats, or deviating their gaze. This phase assessed the system's ability to detect irregular states of attention during study. The results for one of the participants are shown in **Figure 5** [68–72].

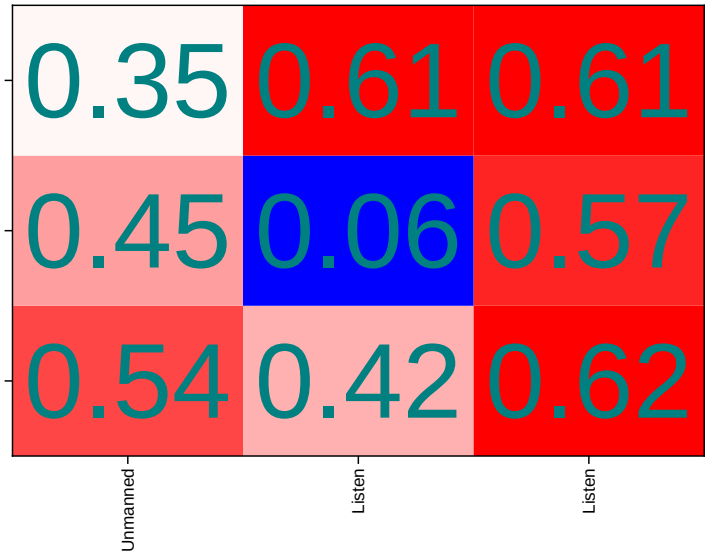

Figure 5. Confusion matrix plot of detection accuracy.

The overall teaching quality of the students is analyzed by combining head posture and expression recognition to calculate the level of attention, engagement, and confusion in the classroom. For the teacher to visualize the classroom situation, the system is represented visually in the form of a bar chart. If the system analyzes that the students' attention, participation, and confusion are low in the classroom learning process, it indicates that the current learning efficiency is not good, and the teacher needs to adjust the teaching strategy to improve the teaching content to enhance the teaching quality.

A system for detecting students' learning attention in an online learning environment that incorporates head posture and line of sight estimation is designed to discriminate subjects' attention using a combination of feature information obtained from head posture and line of sight estimation algorithms. Experiments with multiple subjects show that the system can objectively and accurately identify and analyze students' learning attention.

3.2. Multi-granularity sentiment AI classification model performance

The EEG electrodes with greater emotional relevance are distributed along the edges of the head, particularly at the front and sides, whereas the central region provides relatively less emotional information. This demonstrates that the location of EEG electrodes has a significant impact on emotional classification. Additionally, differential entropy (DE) feature maps derived from EEG signals vary across different frequency bands, indicating the importance of separating information from each frequency band. In this approach, multi-channel, multi-band feature maps are constructed, and a convolutional neural network (CNN) is used for autonomous learning to extract abstract emotional features [73].

The trends in multi-channel EEG DE features over time are depicted in **Figure 6**. Overall, EEG features for the same emotion do not exhibit large changes over time. However, individual channel electrodes do show significant variations in EEG features. Channels with larger variations are likely to contain rich emotional information. Therefore, in this chapter, the temporal information of the same emotion

is fed into the CNN model to allow it to learn from richer empirical data, which in turn enhances the generalization performance of the neural network model [74,75].

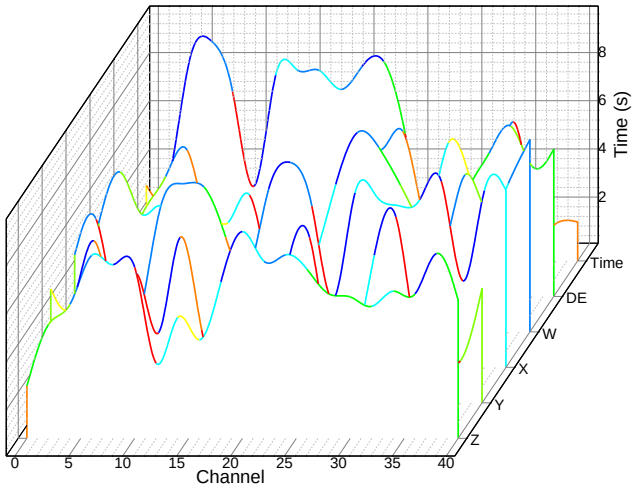

Figure 6. Feature change map.

The training process of the regional user sentiment recognition model is as follows: Read the upper four model layers of the trained model with parameters; this part of the parameters is not trainable. Add two fully connected layers with randomly initialized weight parameters; this part of the parameters is open for training. The data from DEAP were randomly divided into four groups of eight each. The first 40 s of data were used for training, and the last 20 s of data were used for testing. A new model is first trained directly with this dataset to serve as a control, followed by a migration learning model to propose a real-time sentiment recognition model based on migration learning and deep learning on the cloud side. By migrating the generic model trained in the cloud to a small dataset of individuals collected by the edge server, personalized sentiment recognition models can be obtained by training. To improve the recognition accuracy, the edge server periodically collects the sentiment data of users and updates the sentiment recognition model.

The overall emotional state transfer of the robot after external stimulation is better, especially for the happy, sad, surprised, and calm types of emotional state transfer. This experiment proves that the emotional interaction model proposed in this paper can better analyze the emotional state transfer process of the robot, which is conducive to a more natural and harmonious human-robot interaction experience. By calculating the emotion recognition rate as the evaluation performance index and using the leave-one-out cross-validation method to count the experimental results of each algorithm, as shown in **Figure 7**.

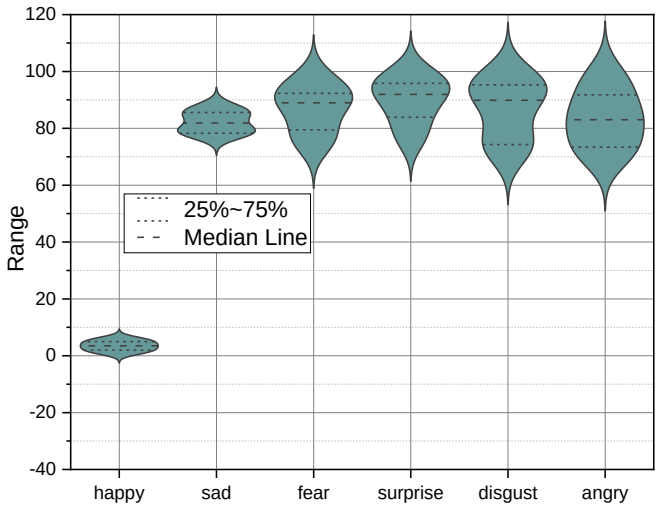

Figure 7. Performance comparison in cross-domain datasets.

The algorithm proposed in this paper demonstrates the best sentiment recognition rate and exhibits significant superiority over other methods. This improvement in recognition rate can be attributed to the feature migration learning capability of the algorithm. By performing difference analysis during feature extraction, the algorithm selectively retains commonality in features and discards information that significantly differs from the target domain. This selective training enhances the recognition rate in the target domain [76]. In contrast, other comparison algorithms lack migration learning capabilities, meaning they incorporate all feature information in the dataset. This inclusion of disordered and irrelevant features leads to a chaotic feature space distribution, ultimately decreasing the sentiment recognition rate [77].

The proposed algorithm effectively addresses the challenge of sentiment recognition by leveraging feature migration learning. By filtering out irrelevant features and focusing on shared feature information, the algorithm not only improves the recognition rate but also offers significant generalization capabilities in the target domain. This approach outperforms traditional methods that do not incorporate feature migration learning, which often suffer from poor recognition rates due to cluttered feature spaces. Overall, this algorithm holds great potential for applications in sentiment analysis and emotion recognition, providing a robust framework for enhancing sentiment classification tasks.

4. Discussion

This paper explores the use of brain-computer interface (BCI) systems for detecting attention fatigue and classifying emotional states, highlighting their immense potential in mental health applications. BCI technology facilitates non-invasive monitoring of brain activity, which is particularly useful for real-time assessments of emotional and cognitive states. EEG signals provide critical insights into mental states, especially through observations of the theta and gamma frequency bands, which are strongly associated with attention and emotion regulation [78,79]. Studies have demonstrated that integrating BCI systems in classroom environments can provide significant insights into student engagement levels, enabling educators to adapt teaching methods based on real-time feedback [80]. Furthermore, the continuous

monitoring of attention levels offers valuable applications in clinical settings, where attention fatigue often correlates with various mental health disorders [81].

The design of a multi-grain emotional AI classification model enhances the accuracy of emotion detection by analyzing EEG signals across different frequency bands. By leveraging differential entropy (DE) features, the model captures both coarse- and fine-grained emotional cues from brain activity. This multichannel approach ensures the accurate identification of emotional states, such as joy, anger, or sadness, even across varying contexts. Recent studies have validated the effectiveness of using convolutional neural networks (CNNs) to process these multi-grain features, particularly in applications requiring real-time classification, such as gaming or interactive learning environments [82,83]. Additionally, the capability to process these signals in near real-time significantly increases the potential of BCIs in scenarios where timely responses are critical, such as emergency medical situations or high-stress professional environments [84].

A key advancement in the field of emotion recognition is the implementation of transfer learning. Transfer learning enables emotion classification models to adapt to new users by transferring knowledge learned from one dataset or individual to another. This is especially beneficial for EEG-based emotion recognition, where inter-subject variability often causes degraded performance in traditional machine learning models [85,86]. By applying transfer learning techniques, models can identify shared features across subjects while discarding irrelevant data, thereby improving generalization performance. This approach has been shown to enhance accuracy in cross-subject settings, particularly in studies involving large, diverse datasets, as demonstrated in multi-domain emotion recognition research [87]. The ability to adapt in real time makes transfer learning an essential component of personalized emotion recognition systems, with promising applications in mental health monitoring, gaming, and education [88].

The future of BCI-based emotion recognition systems lies in developing more sophisticated hybrid models that combine traditional neural networks with advanced deep learning architectures. For example, researchers are exploring the integration of Recurrent Neural Networks (RNNs) with CNNs to improve the temporal processing capabilities of these models, which are critical for tracking dynamic emotional changes over time [89]. Additionally, the application of reinforcement learning in BCI systems could enable the creation of adaptive and autonomous emotion recognition models that continuously learn from new data inputs, further enhancing accuracy and usability in long-term applications [90]. Ultimately, the development of these advanced models will lead to more robust, real-time emotion classification systems, with transformative benefits across fields such as healthcare, education, and entertainment [91–94].

5. Conclusion and future outlook

5.1. Conclusion

In this paper, we leveraged the fractal characteristics of EEG signals as feature values to achieve offline recognition of emotional states. While the experimental results were promising, a considerable gap remains between the controlled

experimental environment and real-world applications. For instance, the use of a 64-conductor EEG acquisition cap, while effective in laboratory settings, poses significant challenges for practical, everyday use due to its complexity and lack of convenience. Additionally, the offline nature of signal processing introduces limitations, as most real-time emotion recognition applications require high-speed processing with minimal computational latency. The computational demands associated with real-time EEG signal processing and the optimization of classification algorithm parameters remain areas in need of further exploration. This study relied heavily on existing parameters from prior research, necessitating deeper comparative analysis and fine-tuning to ensure optimal performance across different contexts. These challenges represent key obstacles that must be addressed before transitioning from experimental analysis to practical applications of emotion recognition systems.

The proposed algorithm for detecting learner fatigue in online learning environments also demonstrated considerable promise, particularly through its integration of head posture detection and vision deviation detection. By calculating the ratio of frames with head or gaze deviation to the total number of frames within a given time period, the system successfully identified inattentive behaviors, such as gaze aversion and distraction. The attention detection experiment yielded excellent performance, highlighting the potential of the system to improve educational outcomes by identifying and addressing student engagement issues in real-time.

5.2. Future outlook

Looking ahead, several critical advancements are necessary to enhance the applicability and effectiveness of EEG-based emotion recognition and attention detection systems.

First, improvements in wearable EEG technology will be essential for making real-time emotional and cognitive monitoring more practical. The transition from bulky 64-conductor systems to more compact, user-friendly, and less obtrusive wearables is a critical step toward widespread adoption in real-world settings, such as education, healthcare, and daily life applications [78–81].

Second, advancements in real-time processing algorithms are needed to address the computational challenges posed by EEG data. Integrating deep learning techniques—such as convolutional and recurrent neural networks—with edge computing capabilities could enable faster and more efficient processing of emotional and cognitive signals, making real-time applications more feasible [82–85]. Moreover, optimizing transfer learning models to account for individual variability and cross-domain applications will ensure these systems remain adaptable across different user profiles and contexts [86–88].

Lastly, enhancing the system's generalization capabilities is vital to improving its robustness against various environmental factors, such as lighting conditions, movement, and external noise. Future research should prioritize multi-modal approaches that combine EEG data with other bio-signals, such as facial expressions, heart rate, or eye movements. By integrating these complementary data sources, researchers can develop more accurate and reliable emotion recognition models better suited to complex, real-world environments [89–91].

By addressing these challenges, the next generation of emotion recognition and attention detection systems will not only become more accurate but also more accessible, adaptable, and seamlessly integrated into everyday life. These advancements will pave the way for transformative applications in education, healthcare, and beyond, fostering improved mental well-being and engagement across diverse contexts.

Ethical approval: Not applicable.

Conflict of interest: The author declares no conflict of interest.

References

1. Mesquita B. Between us: How cultures create emotions. WW Norton & Company; 2022.
2. Leong SC, Tang YM, Lai CH, et al. Facial expression and body gesture emotion recognition: A systematic review on the use of visual data in affective computing. Computer Science Review. 2023; 48: 100545.
3. Yeh SC, Wu EHK, Lee YR, et al. User experience of virtual-reality interactive interfaces: A comparison between hand gesture recognition and joystick control for xrspace manova. Applied Sciences. 2022; 12(23): 12230.
4. Myers MH. Automatic detection of a student's affective states for intelligent teaching systems. Brain Sciences. 2021; 11(3): 331.
5. Xia J, Zhang H, Wen S, et al. An efficient multitask neural network for face alignment, head pose estimation and face tracking. Expert Systems with Applications. 2022; 205: 117368.
6. Zad S, Heidari M, James Jr H, et al. Emotion detection of textual data: An interdisciplinary survey. In: Proceedings of the 2021 World AI IoT Congress (AIIoT); 10–13 May 2021; Seattle, WA, United States.
7. Szymkowiak A, Gaczek P, Jeganathan K, et al. The impact of emotions on shopping behavior during epidemic. What a business can do to protect customers. Journal of Consumer Behaviour. 2021; 20(1): 48–60.
8. Zhang J, Wang M. A survey on robots controlled by motor imagery brain-computer interfaces. Cognitive Robotics. 2021; 1: 12–24.
9. Singh P, Dalal D, Vashishtha G, et al. Learning Robust Deep Visual Representations from EEG Brain Recordings. In: Proceedings of the IEEE/CVF Winter Conference on Applications of Computer Vision; 4–8 Jan 2024; Waikoloa, HI, USA. pp. 7553–7562.
10. Stajić T, Jovanović J, Jovanović N, et al. Emotion recognition based on DEAP database physiological signals. In: Proceedings of the 2021 29th telecommunications forum (TELFOR); 23–24 November 2021; Belgrade, Serbia. pp. 1–4.
11. Javaid MM, Yousaf MA, Sheikh QZ, et al. Real-time EEG-based human emotion recognition. In: Proceedings of the International Conference on Neural Information Processing, ICONIP 2015; 9–12 November 2015; Istanbul, Turkey. pp. 182–190.
12. Naser DS, Saha G. Influence of music liking on EEG based emotion recognition. Biomedical Signal Processing and Control. 2021; 64: 102251.
13. LeCun Y, Bengio Y, Hinton G. Deep learning. Nature. 2015; 521: 436–444.
14. Elyamany O, Leicht G, Herrmann CS, et al. Transcranial alternating current stimulation (tACS): From basic mechanisms towards first applications in psychiatry. European Archives of Psychiatry and Clinical Neuroscience. 2021; 271(1): 135–156.
15. Lambay A, Liu Y, Morgan PL, et al. Machine learning assisted human fatigue detection, monitoring, and recovery. Digital Engineering. 2024; 1: 100004.
16. Gonzalez-Izal M, Malanda A, Gorostiaga E, et al. Electromyographic models to assess muscle fatigue. Journal of Electromyography and Kinesiology. 2012.
17. Chaddad A, Wu Y, Kateb R, et al. Electroencephalography signal processing: A comprehensive review and analysis of methods and techniques. Sensors. 2023; 23(14): 6434.
18. Deligani RJ, Borgheai SB, McLinden J, et al. Multimodal fusion of EEG-fNIRS: A mutual information-based hybrid classification framework. Biomed Opt Express. 2021; 12(3): 1635–1650.

19. Zhai J, Barreto A. Stress recognition using non-invasive technology. In: Proceedings of the Nineteenth International Florida Artificial Intelligence Research Society Conference (FLAIRS 2006); 11–13 May 2006; Melbourne Beach, FL, USA.
20. Tzimiropoulos G, Zafeiriou S, Pantic M. Robust and efficient parametric face alignment. In: Proceedings of the 2011 International Conference on Computer Vision (ICCV); 06–13 November 2011; Barcelona, Spain.
21. Wright J, Yang A, Ganesh A, et al. Robust face recognition via sparse representation. IEEE Transactions on Pattern Analysis and Machine Intelligence. 2009; 31(2): 210–227.
22. Garcia-Blancas J, Dominguez-Ramirez OA, Rodriguez-Torres EE, et al. A technological proposal for a robot brain computer interface for neurorehabilitation purposes. The European Physical Journal Special Topics. 2025; 1–29.
23. Henry JC. Electroencephalography: Basic principles, clinical applications, and related fields. Neurology. 2006; 67(11).
24. Fermaglich J. Electric fields of the brain: The neurophysics of EEG. JAMA. 1982; 247(13): 1879–1880.
25. Kim J, André E. Emotion recognition based on physiological changes in music listening. IEEE Transactions on Pattern Analysis and Machine Intelligence. 2008; 30(12): 2067–2083.
26. Müller-Putz GR, Scherer R, Brunner C, et al. Better than random: A closer look on BCI results. International Journal of Bioelectromagnetism. 2008; 20(1): 52–55.
27. Ang KK, Guan C, Chua KS, et al. A clinical study of motor imagery-based brain-computer interface for upper limb robotic rehabilitation. In: Proceedings of the 2009 Annual International Conference of the IEEE Engineering in Medicine and Biology Society; 3–6 September 2009; Minneapolis, MN, USA.
28. Nunez PL, Srinivasan R. Electric Fields of the Brain: The Neurophysics of EEG. Oxford University Press; 2006.
29. Zhang H, Zhou QQ, Chen H, et al. The applied principles of EEG analysis methods in neuroscience and clinical neurology. Military Medical Research. 2023; 10(1): 67.
30. Gong ZQ, Gao P, Jiang C, et al. DREAM: A toolbox to decode rhythms of the brain system[J]. Neuroinformatics. 2021; 19: 529–545.
31. Wang XJ. Neurophysiological and computational principles of cortical rhythms in cognition. Physiological Reviews. 2010.
32. Ranjan R, Sahana BC, Bhandari AK. Ocular artifact elimination from electroencephalography signals: A systematic review. Biocybernetics and Biomedical Engineering. 2021; 41(3): 960–996.
33. Gratton G, Coles MG, Donchin E. A new method for off-line removal of ocular artifact. Electroencephalography and Clinical Neurophysiology. 1983.
34. Birnie MT, Baram TZ. Principles of emotional brain circuit maturation. Science. 2022; 376(6597): 1055–1056.
35. Alsharif AH, Salleh NZM, Baharun R. The neural correlates of emotion in decision-making. International journal of academic research in business and social sciences. 2021; 11(7): 64–77.
36. MacLean PD. The triune brain in evolution: Role in paleocerebral functions. Plenum Press; 1990.
37. Swanson LW. Brain Architecture: Understanding the Basic Plan. Oxford University Press; 2012.
38. De Luca CJ, Gilmore LD, Kuznetsov M, et al. Filtering the surface EMG signal: Movement artifact and baseline noise contamination. Journal of Biomechanics. 2010.
39. Merletti R, Farina D. Surface Electromyography: Physiology, Engineering, and Applications. IEEE Press/Wiley; 2016.
40. Phinyomark A, Limsakul C, Phukpattaranont P. A review of control methods for electromyography pattern classification. Expert Systems with Applications. 2013.
41. Reaz MB, Hussain MS, Mohd-Yasin F. Techniques of EMG signal analysis: Detection, processing, classification, and applications. Biological Procedures Online. 2006.
42. Konrad P. The ABC of EMG: A Practical Introduction to Kinesiological Electromyography. Noraxon. 2005.
43. Webster JG. Medical Instrumentation: Application and Design. John Wiley & Sons; 2009.
44. De Luca CJ. Surface electromyography: Detection and recording. Delsys Incorporated; 2002.
45. Merletti R, Farina D. Analysis of intramuscular electromyographic signals. Philosophical Transactions of the Royal Society B: Biological Sciences. 2009.
46. Butterworth S. On the theory of filter amplifiers. Experimental Wireless and the Wireless Engineer. 1930.
47. Franco S. Design with operational amplifiers and analog integrated circuits. McGraw-Hill Education; 2014.
48. Huigen E, Peper A, Grimbergen CA. Investigation into the origin of the noise of surface electrodes. Medical and Biological Engineering and Computing. 2002.
49. Russell JA. A circumplex model of affect. Journal of Personality and Social Psychology. 1980.

50. Lang PJ, Bradley MM, Cuthbert BN. International affective picture system (IAPS): Affective ratings of pictures and instruction manual. University of Florida; 2008.
51. Posner J, Russell JA, Peterson BS. The circumplex model of affect: An integrative approach to affective neuroscience, cognitive development, and psychopathology. Development and Psychopathology. 2005.
52. Tan C, Sun F, Kong T, et al. A survey on deep transfer learning. In: Proceedings of the 27th International Conference on Artificial Neural Networks; 4–7 October 2018; Rhodes, Greece. pp. 270–279.
53. Blankertz B, Tomioka R, Lemm S, et al. Optimizing spatial filters for robust EEG single-trial analysis. IEEE Signal Processing Magazine. 2008.
54. Lu Z, Lin J, Shen Z. Kernel-based feature extraction for time-varying EEG signal classification. Neurocomputing. 2014.
55. Wu W, Gao S, Hong B, et al. Classifying single-trial EEG during motor imagery by iterative spatio-spectral patterns learning (ISSPL). IEEE Transactions on Biomedical Engineering. 2008.
56. Rakotomamonjy A, Guigue V. BCI competition III: Dataset II- ensemble of SVMs for BCI P300 speller. IEEE Transactions on Biomedical Engineering. 2008.
57. Lotte F, Congedo M, Lécuyer A, et al. A review of classification algorithms for EEG-based brain-computer interfaces. Journal of Neural Engineering. 2007.
58. Zhang D, Meng H, Wang Z, et al. Head pose estimation based on deep learning in classroom scenarios. Neurocomputing. 2020.
59. Asteriadis S, Karpouzis K, Kollias S. Head pose estimation for perceptual human-computer interfaces: A survey. Cognitive Computation. 2011.
60. Lucey P, Cohn JF, Matthews I, et al. Automatically detecting pain in video through facial action units. IEEE Transactions on Systems, Man, and Cybernetics, Part B (Cybernetics). 2010; 41(3): 664–674.
61. D'mello SK, Kory J. A review and meta-analysis of multimodal affect detection systems. ACM computing surveys (CSUR). 2015; 47(3): 1–36.
62. Tziortziotis N, Asteriadis S, Karpouzis K, et al. A neuro-inspired attention model for classroom attention monitoring using a head pose estimation system. Pattern Recognition Letters. 2012.
63. Mohamad Nezami O, Dras M, Hamey L, et al. Automatic recognition of student engagement using deep learning and facial expression. In: Proceedings of the Joint European Conference on Machine Learning and Knowledge Discovery in Databases; 14–18 September 2020; Ghent, Belgium. pp. 273–289.
64. Zaletelj J, Košir A. Predicting students' attention in the classroom from Kinect facial and body features. EURASIP Journal on Image and Video Processing. 2017.
65. Bosch N, D'Mello S, Mills C, et al. Using video to automatically detect learner affect in computer-enabled classrooms. ACM Transactions on Interactive Intelligent Systems (TiiS). 2016.
66. Zhang Z, Sugano Y, Fritz M, et al. It's written all over your face: Full-face appearance-based gaze estimation. In: Proceedings of the IEEE Conference on Computer Vision and Pattern Recognition; 21–26 July 2017; Honolulu, HI, USA.
67. Krafka K, Khosla A, Kellnhofer P, et al. Eye tracking for everyone. In: Proceedings of the 2016 IEEE Conference on Computer Vision and Pattern Recognition (CVPR); 27–30 June 2016; Las Vegas, NV, USA.
68. D'Mello SK, Graesser AC. Multimodal semi-automated affect detection from conversational cues, gross body language, and facial features. User Modeling and User-Adapted Interaction. 2010; 20: 147–187.
69. Whitehill J, Serpell Z, Lin YC, et al. The faces of engagement: Automatic recognition of student engagement from facial expressions. IEEE Transactions on Affective Computing. 2014; 5(1): 86–98.
70. Abadi M, Khosla A, Ramaswamy H, et al. TensorFlow: A system for large-scale machine learning. In: Proceedings of the 12th USENIX Conference on Operating Systems Design and Implementation (OSDI); 2–4 November 2016; Savannah, GA, USA.
71. Xia L, Li Y, Cai X, et al. Collaborative contrastive learning for cross-domain gaze estimation[J]. Pattern Recognition, 2025, 161: 111244.
72. Košir A, Zaletelj J. Classroom attention monitoring system based on facial and body movements using Kinect. EURASIP Journal on Image and Video Processing. 2017.
73. Lin YP, Wang CH, Wu TL, et al. EEG-based emotion recognition in music listening: A comparison of schemes for multiclass support vector machine. In: Proceedings of the IEEE International Conference on Acoustics, Speech and Signal Processing (ICASSP); 19–24 April 2009; Taipei, Taiwan, China.

74. Zaidi SR, Khan NA, Hasan MA. Bridging Neuroscience and Machine Learning: A Gender-Based Electroencephalogram Framework for Guilt Emotion Identification[J]. Sensors, 2025, 25(4): 1222.
75. Craik A, He Y, Contreras-Vidal JL. Deep learning for electroencephalogram (EEG) classification tasks: A review. Journal of neural engineering. 2019; 16(3): 031001.
76. Pan SJ, Yang Q. A comprehensive survey on transfer learning. IEEE Transactions on Knowledge and Data Engineering. 2010; 22(10): 1345–1359.
77. Chato L, Regentova E. Survey of transfer learning approaches in the machine learning of digital health sensing data. Journal of Personalized Medicine. 2023; 13(12): 1703.
78. Brouwer AM, Hogervorst MA, van Erp JB, et al. Estimating workload using EEG spectral power and ERPs in the n-back task. Journal of Neural Engineering. 2012.
79. Borghini G, Arico P, Di Flumeri G, et al. A neurophysiological training evaluation metric for the implementation of personalized neurometrics. Frontiers in Human Neuroscience. 2017.
80. Mahmoudi A, Khosrotabar M, Gramann K, et al. Using passive BCI for personalization of assistive wearable devices: a proof-of-concept study[J]. IEEE Transactions on Neural Systems and Rehabilitation Engineering, 2025.
81. Chavarriaga R, Sobolewski A, Millan JDR. Errare machinale est: The use of error-related potentials in brain-machine interfaces. Frontiers in Neuroscience. 2014.
82. Schirrmeister RT, Springenberg JT, Fiederer LDJ, et al. Deep learning with convolutional neural networks for EEG decoding and visualization. Human Brain Mapping. 2017.
83. Han J, Li H, Zhang X, et al. EMCNN: Fine-Grained Emotion Recognition based on PPG using Multi-scale Convolutional Neural Network[J]. Biomedical Signal Processing and Control, 2025, 105: 107594.
84. Liu Y, Sourina O, Nguyen MK. Real-time EEG-based human emotion recognition and visualization. In: Proceedings of the International Conference on Cyberworlds (CW); 20–22 October 2010; Singapore.
85. Wu D, Xu Y, Lu B. Transfer learning for EEG-based brain-computer interfaces: A Euclidean space data alignment approach. IEEE Transactions on Biomedical Engineering. 2015.
86. Abir S I, Shoha S, Hossain MM, et al. Machine Learning and Deep Learning Techniques for EEG-Based Prediction of Psychiatric Disorders[J]. Journal of Computer Science and Technology Studies, 2025, 7(1): 46–63.
87. Zhang K, Jin R, Zhou ZH. Transfer learning in brain-computer interfaces: A literature review. Journal of Biomedical Informatics. 2020.
88. Chao ZC, Nagasaka Y, Fujii N. Long-term asynchronous decoding of arm motion using electrocorticographic signals in monkeys. Frontiers in Neuroengineering. 2010.
89. Bashivan P, Rish I, Yeasin M, et al. Learning representations from EEG with deep recurrent-convolutional neural networks. In: Proceedings of the International Conference on Learning Representations (ICLR); 2–4 May 2016; San Juan, Puerto Rico.
90. Zhang Y, Zhou G, Jin J, et al. Aggregation of sparse linear discriminant analyses for event-related potential classification in brain-computer interface. International Journal of Neural Systems. 2015.
91. Wang Z, Li S, Luo J, et al. Channel reflection: Knowledge-driven data augmentation for EEG-based brain-computer interfaces. Neural Networks. 2024; 176: 106351. doi: 10.1016/j.neunet.2024.106351
92. Wickramasinghe N, Chalasani S, Sloane E. Digital disruption in healthcare. Springer; 2022.
93. Qi W, Sun S, Niu T, et al. Research and prospects of virtual reality systems applying exoskeleton technology. Universal Access in the Information Society. 2024; 23(1): 119–140.
94. Stasieńko JAN, Dytman-Stasieńko A, Madej K, et al. Representations of Disability in Video Games. Available from: https://d1wqtxts1xzle7.cloudfront.net/88357265/Fragile_Avatars_ebook1-libre.pdf?1658378810=&response-content-disposition=inline%3B+filename%3DFragile_Avatars_Representations_of_Disa.pdf&Expires=1740626375&Signature=fT1ftgfLkm3Oua-Hh7NMIzsyog96U5JWUxhKEiqOCeTb56YIdSHVQfhPZeg9Ig7XnueVxdZXjGEpsKrRBYqnpJar5qSV84Ix6tCRUKzXyB60BQii7V6Q0Ko6KQQSlB7q9YHo4BwOSp-NwCiRjrbQYUhw7JRjPT3sQExf34GvtypQlAL~dvVVq2oZisknXDVkpnZ7hskL7gifUSM6qsJYufi3dmqbsA71oqZChDGceRqazY5~RRD3kPTkU1Gc5cQKFlCkAy6S6eGFlpGFWWHU1pK6egw35C72DjGAonEabic25xzuGi2lq1-y-ti1wwYuf8GVi4CK51gth7lMQXLTJQ__&Key-Pair-Id=APKAJLOHF5GGSLRBV4ZA (accessed on 28 November 2024).